Pulmonary nodule detection in PET/CT images: Improved approach using combined nodule detection and hybrid FP reduction

Atsushi Teramoto*[a], Hiroshi Fujita[b], Yoya Tomita[c], Katsuaki Takahashi[c], Osamu Yamamuro[c], Tsuneo Tamaki[c],

[a] Faculty of Radiological Technology, School of Health Sciences, Fujita Health University, 1-98 Dengakugakubo, Kutsukake-cho, Toyoake-city, Aichi 470-1192, Japan;
[b] Department of Intelligent Image Information, Division of Regeneration and Advanced Medical Sciences, Graduate School of Medicine, Gifu University, 1-1 Yanagido, Gifu 501-1194, Japan;
[c] East Nagoya Imaging Diagnosis Center, 3-4-26 Jiyugaoka, Chikusa-ku, Nagoya 464-0044, Japan;

ABSTRACT

In this study, an automated scheme for detecting pulmonary nodules in PET/CT images has been proposed using combined detection and hybrid false-positive (FP) reduction techniques. The initial nodule candidates were detected separately from CT and PET images. FPs were then eliminated in the initial candidates by using support vector machine with characteristic values obtained from CT and PET images. In the experiment, we evaluated proposed method using 105 cases of PET/CT images that were obtained in the cancer-screening program. We evaluated true positive fraction (TPF) and FP / case. As a result, TPFs of CT and PET detections were 0.76 and 0.44, respectively. However, by integrating the both results, TPF was reached to 0.82 with 5.14 FPs/case. These results indicate that our method may be of practical use for the detection of pulmonary nodules using PET/CT images.

Keywords: PET, CT, Computer-aided detection (CAD), Lung nodule

1. INTRODUCTION

Lung cancer is the leading cause of death among males in the world and its incidence is continuing to increase. To reduce lung-cancer-related deaths, it is necessary to detect and treat the cancer at an early stage. Recently, PET/CT has been adopted as a mass-screening tool for cancer diagnosis, because it improves the ability to detect tumors at an early stage. PET/CT combines in a single system both a PET and a CT, so that images acquired from both devices can be taken sequentially, in the same section from the patient. Thus, functional imaging obtained by PET, which depicts the spatial distribution of metabolic or biochemical activity in the body can be more precisely aligned. X-ray CT has anatomical information; it is used for lung nodule detection widely [1-3]. X-ray CT image compensates the anatomical information, which is lacking from the pure PET system.

However, PET/CT generates a large number of images that must be manually examined by a radiologist, and therefore, it is necessary to reduce this load. Computer-aided detection (CAD) provides a computer output as a 'second opinion' to assist radiologists in diagnosing various diseases from medical images. We

* teramoto@fujita-hu.ac.jp TEL: +81-562-93-9415; FAX: +81-562-93-4595

Medical Imaging 2012: Computer-Aided Diagnosis, edited by Bram van Ginneken, Carol L. Novak,
Proc. of SPIE Vol. 8315, 83152V · © 2012 SPIE · CCC code: 1605-7422/12/$18 · doi: 10.1117/12.912102

focus on the lung nodule detection using whole-body PET/CT images. With regard to the detection of lung nodules, many researchers have developed CAD schemes using CT [4-9] or PET [10] images. We had proposed novel CAD scheme for nodule detection using both CT and PET images [11].

In this study, we propose the improved detection scheme using combined detection and hybrid false positive (FP) reduction for nodule detection in PET/CT images.

2. METHODS

2.1 Image dataset

Dataset consisted of 105 Japanese men and women with whole body PET/CT images from 2009 to 2010, scanned for the purpose of cancer screening program. The PET/CT images were scanned using SIEMENS unit (Truepoint Biograph 40) and were scanned using standard settings routinely used clinically. The spatial resolution of the PET image was $4.0 \times 4.0 \times 2.0$ mm^3 and that of the CT image was $0.97 \times 0.97 \times 2.0$ mm^3. There were 221 nodules in 84 abnormal cases. 54 cases were randomly picked up for training of proposed scheme and optimizing their internal parameters. The remaining 51 cases are for testing. This study was approved by our institutional review board.

2.2 Method overview

An overview of the method developed for nodule detection in PET/CT images is shown in Fig. 1. Using the proposed scheme, first, the pulmonary nodules were detected from the given PET and CT images separately, using specific features of each image. Subsequently, FPs in the initial candidates are eliminated using hybrid FP reduction technique. Finally, nodule candidate regions were obtained. The detection and integration methods are described as follows.

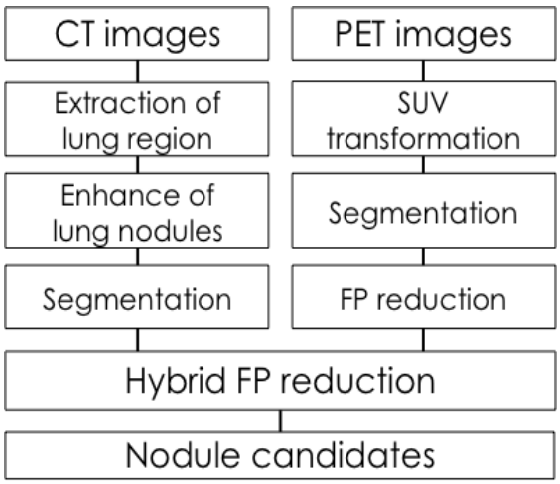

Fig. 1 An overview of the proposed detection method. The results from the CT and PET images are combined, and FPs are eliminated by hybrid FP reduction technique to give an automated detection of pulmonary nodules.

2.3 Detection using CT images

In the detection using CT, the lung region is detected and a nodule in the lung region is enhanced using a cylindrical filter we developed [8]. The enhanced image is binarized, and then, initial nodule candidates are obtained using three-dimensional (3D) labeling.

2.4 Detection using PET images

In the detection using PET, image is binarized using a predetermined threshold. In this study, the pixel value in which the standard uptake value (SUV [12]) became 2.0 is selected as a threshold. Then, 3D labeling is applied to the binary image, in order to distinguish the highly uptake regions. FPs outside the lung region are eliminated using extracted lung region determined by the CT images.

2.5 Hybrid FP reduction

After detecting initial nodule candidates as described above, combined results are obtained by logic OR. However, there are approx. 30 FPs per case in the initial combined results. Therefore, FPs are eliminated using the characteristic features obtained from CT and PET images. FP elimination is conducted using rule-based classifier followed by two support vector machine classifiers.

A. Rule-based classifier

Rule-based classifier identifies the explicit TPs and FPs based on properties of nodule candidates as follows.

(1) Candidates detected by PET alone are judged as TPs.
(2) Candidates whose SUV value is higher than 10.0 are judged as TPs.
(3) Candidates whose vector concentration value is less than 0.5 are judged as FPs.

B. SVM classifiers

Remaining candidate regions processed above method are then processed by two SVM classifiers.

SVM #1: Candidates detected only by CT images are given to SVM#1. TPs and FPs are classified using 20 characteristic features.

SVM #2: Candidates detected by both CT and PET images are classified by SVM #2 using 26 characteristic features.

3. EXPERIMENTS

The detection parameters were determined using the training dataset comprising PET/CT images of 53 cases. For an objective evaluation of the efficacy of our method for unseen cases, our method was applied to 52 other images. During this evaluation, the true-positive fraction (TPF) and the number of false positives per case (FPs/case) were calculated.

Regarding the detection parameters, filter radiuses of CF were set at 5,10, 15, 20, 25 mm, highest output of filter is output as nodule enhanced image. For PET detection, threshold for detection was set at 2.0. In SVM for FP reduction, we introduced the LibSVM [13]; C-SVC with the kernel of the 3rd polynomial function was introduced. These data were processed using a 2.8 GHz core i7 CPU with a 4.0 GB memory.

Table 1 shows the result of TPF and FP/case using the 52 cases of the evaluation dataset. The TPF for detecting nodules using only CT images was 0.76, and FP/case was 5.27. Using PET, detection capability of the initial nodule candidate was as follows: TPF = 0.44 and FP/case = 0.66. By combining the 2 results, the TPF was improved to 0.82 with an FP/case of 5.11. Therefore, the sensitivity of our hybrid scheme is better than that of the independent detection systems using only CT or PET images.

Figures 2,3,and 4 show the results that nodules were detected correctly. In Fig.2(b), PET image does not have high metabolic information. However, CT image has three nodules in left upper lobe (Fig.2(a)); proposed method detected the nodule using CT image as solid rectangles in Fig.2(a). In Fig.3(a), nodule was not detected using CT image because the nodule adhered to the blood vessels. On the other hand, nodule was detected using PET image (Fig.3(b)) as shown by dashed rectangle since nodule has highly uptake. Figure 4 shows the nodule detected by both PET and CT images. Regions detected are shown as double-lined box; they can be used as more reliable results.

Thus, owing to the integration of the detection results of 2 different types of imaging modalities, the sensitivity of our hybrid scheme is higher than that of independent detection systems using only CT or PET.

Table 1. Evaluation result

	CT detection	PET detection	Combined
TPF	0.76	0.44	0.82
FPs/case	5.27	0.66	5.14

4. CONCLUSIONS

In this study, we have proposed an automated scheme for detecting pulmonary nodules in PET/CT images using combined detection and hybrid FP reduction techniques. Proposed method detects the lung nodule from both CT and PET images. As for the detection in CT images, solitary nodules are detected using Cylindrical Filter that we developed. PET images are binarized based on standard uptake value (SUV); highly uptake regions are detected. FPs in initial candidates were then eliminated in the initial candidates by using support vector machine with characteristic features obtained from CT and PET images. In the experiments, we evaluated proposed method using 105 cases of PET/CT images obtained for the cancer-screening program. We found that the sensitivity of our scheme was 0.82 and the FP/case was 5.11; these results are more desirable than those obtained via independent detections using CT or PET. In summary, these results indicate that our method may be useful for the lung cancer detection using PET/CT images.

ACKNOWLEDGMENT

The authors are grateful to M.Nishio, C.Wei-Ping, T.Kobayashi, and S.Tamai from Nagoya Radiological Diagnosis Center, N.Hayashi from Fujita Health University. This work is in part supported by "Computational Anatomy for Computer-aided Diagnosis and Therapy: Frontiers of Medical Image Sciences" funded by Grant-in-Aid for Scientific Research on Innovative Areas, MEXT, Japan.

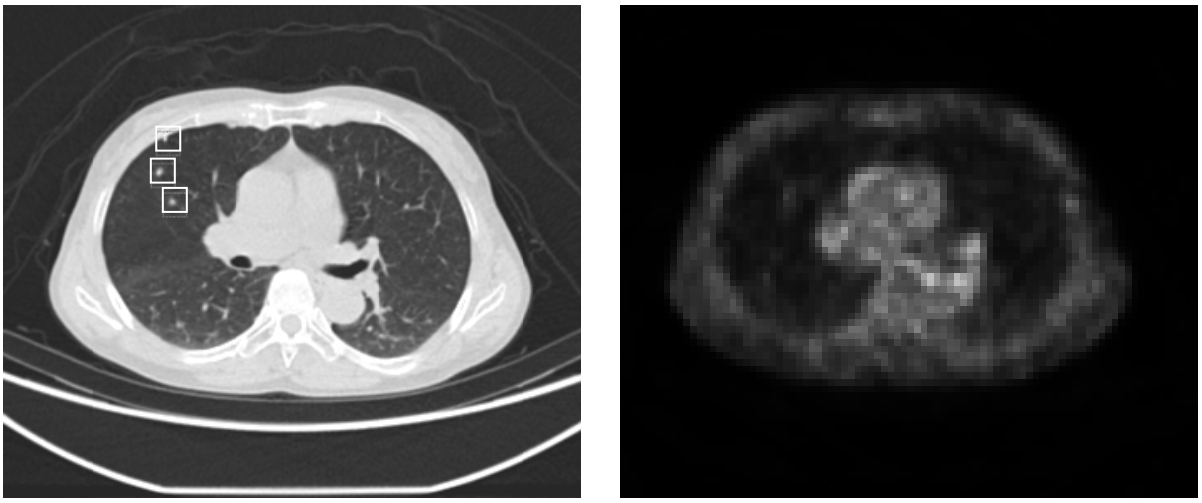

(a) CT image (b) PET image

Figure 2. Nodule detected by CT image. Box indicates the nodules detected by the proposed method. PET image does not provide strong metabolic information. However, the CT image shows three < 1 cm nodules in the right-upper lobe; using our method, we detected the nodule using the CT images.

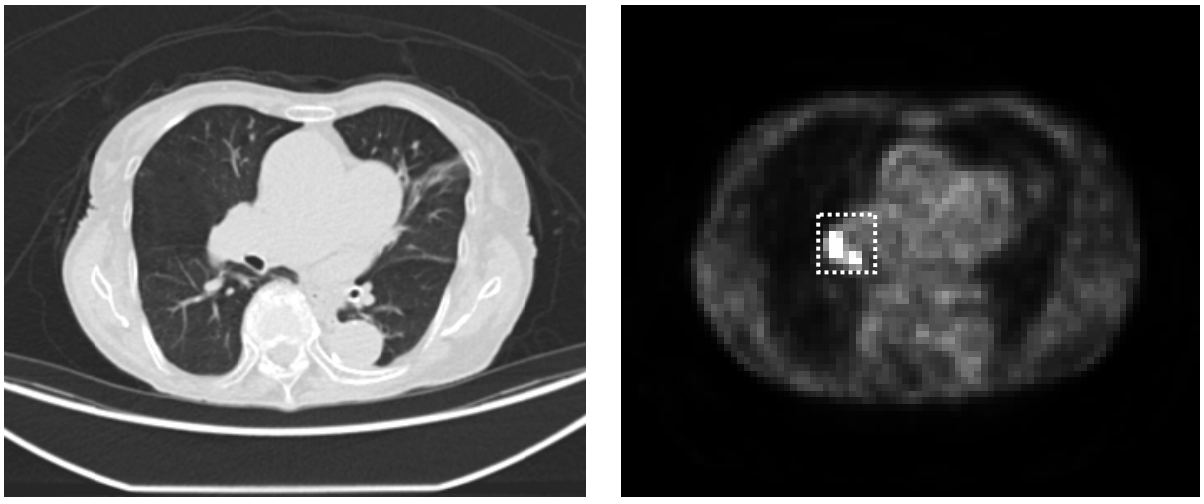

(a) CT image (b) PET image

Figure 3. Nodule detected by PET image. In the CT image, the nodule was not detected because it adhered to the blood vessel. It was detected using the PET image since the nodule has a high uptake.

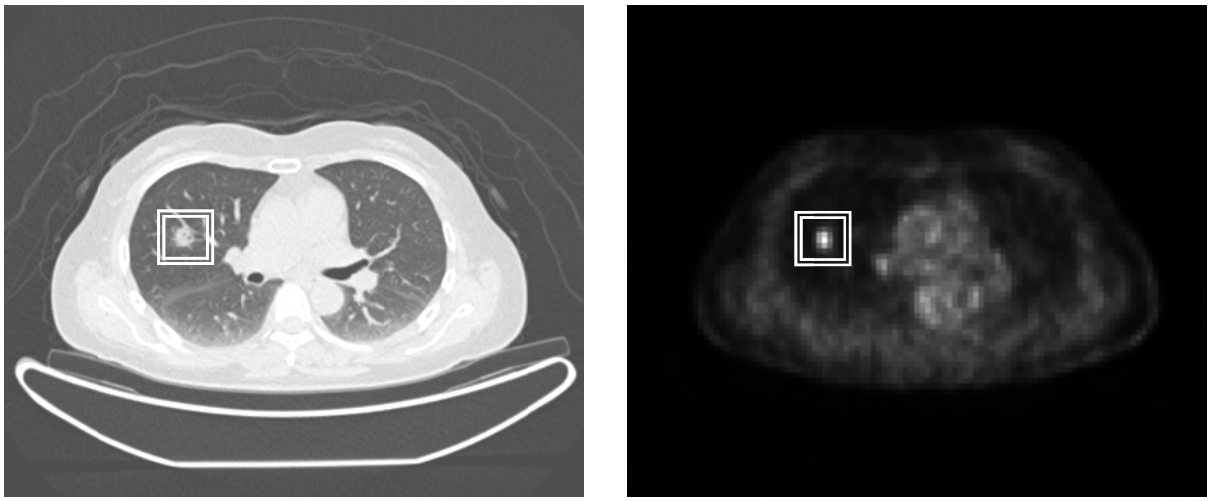

(a) CT image (b) PET image

Figure 4. Nodule detected by CT and PET images. Double lined boxes indicate the nodules detected by the proposed method; they can be used as more reliable results.

References

[1] Sone, S., Takashima, S., Li, F., et al., "Mass screening for lung cancer with mobile spiral computed tomography scanner," The Lancet 351, 1242-1245 (1998).

[2] Ost, D., Fein, A., "Management strategies for the solitary pulmonary nodule," Curr Opin Plum Med, 10(4), 272-278 (2004).

[3] MacMahon, H., Austin, J.H., et al., "Guidelines for management of small pulmonary nodules detected on CT scans: a statement from the Fleischner Society," Radiology 237(2), 395-400 (2005).

[4] Lee, Y., Hara, T., Fujita, H., et al., "Automated detection of pulmonary nodules in herical CT images based on an improved template-matching technique," IEEE Trans Med Imaging 20(7), 595-604 (2001).

[5] Lee, Q., "Recent progress in computer-aided diagnosis of lung nodules on thin-section CT," Computerized Medical Imaging and Graphics 31(4-5), 248-257 (2007).

[6] Opfer, R., Wiemker, R., "Performance analysis for computer-aided lung nodule detection on LIDC data," Proc. of the SPIE - Medical Imaging 2007 6515, 65151C 1-9 (2007).

[7] Li, Q., Li, F., Doi, K., "Computerized detection of lung nodules in thin-section CT images by use of selective enhancement filters and an automated rule-based classifier," Acad Radiol 15(2), 165-175 (2008).

[8] Teramoto, A., Tsuzaka, M., Hara, T., et al., "High-speed detection method of solitary nodules in 3D chest CT images based on cylindrical filter," IEICE Technical Report 108(305), 83-86 (2009).

[9] Messay, T., Hardie, R., Rogers, S., "A new computationally efficient CAD system for pulmonary nodule detection in CT imagery," Medical Image Analysis 14(3),390-406 (2010).

[10] Hara, T., Kobayashi, T., Kawai, K., et al., "Automated scoring system of standard uptake value for torso FDG-PET images," Proc. of SPIE Medical Imaging 2008: Computer-aided diagnosis 6915, 691534-1 - 691534-4 (2008).

[11] Teramoto, A., Fujita, H., Tomita, Y., et al., " Hybrid CAD Scheme for Lung Nodule Detection in PET/CT Images," Proc. of SPIE Medical Imaging 2011: Computer-Aided Diagnosis 7963,796335-1-6 (2011).

[12] John, W., "SUV: Standard uptake or silly uptake value," J Nucl Med 36(10), 1836-1839 (1995).

[13] Chang, C.C., Lin, C.J., "LIBSVM: a library for support vector machines," Software available at http://www.csie.ntu.edu.tw/~cjlin/libsvm/